

AperTO - Archivio Istituzionale Open Access dell'Università di Torino

## B semileptonic moments at NNLO

### **This is the author's manuscript**

*Original Citation:*

*Availability:*

This version is available <http://hdl.handle.net/2318/93417> since

*Published version:*

DOI:10.1007/JHEP09(2011)055

*Terms of use:*

Open Access

Anyone can freely access the full text of works made available as "Open Access". Works made available under a Creative Commons license can be used according to the terms and conditions of said license. Use of all other works requires consent of the right holder (author or publisher) if not exempted from copyright protection by the applicable law.

(Article begins on next page)

# *B* semileptonic moments at NNLO

Paolo Gambino

*Dipartimento di Fisica Teorica, Università di Torino*  
*& INFN, Sezione di Torino, I-10125 Torino, Italy*

## Abstract

The calculation of the moments in inclusive *B* meson semileptonic decays is upgraded to  $O(\alpha_s^2)$ . The first three moments of the lepton energy and invariant hadronic mass distributions are computed for arbitrary cuts on the lepton energy and in various renormalization schemes, finding in general small deviations from the  $O(\alpha_s^2\beta_0)$  calculation. I also review the relation between  $\overline{\text{MS}}$  and kinetic heavy quark masses.

# 1 Introduction

The  $V_{cb}$  element of the Cabibbo-Kobayashi-Maskawa quark mixing matrix is naturally determined in semileptonic  $B$  decays to charmed hadrons. In the case of exclusive final states, like for  $B \rightarrow D^{(*)}\ell\nu$ , the corresponding form factors have to be computed by non-perturbative methods, for instance on the lattice. On the other hand, in the case of inclusive semileptonic decays  $B \rightarrow X_c\ell\nu$  the existence of an Operator Product Expansion (OPE) ensures that non-perturbative effects are suppressed by powers of the bottom mass  $m_b$  and are parameterized by a limited number of matrix elements of local operators which can be extracted from experimental data. The total inclusive width and the first few moments of the kinematic distributions are therefore expected to be well approximated by a double series in  $\alpha_s$  and  $\Lambda_{\text{QCD}}/m_b$  [1, 2]. The general strategy for the inclusive determination of  $|V_{cb}|$  consists in extracting the most important non-perturbative parameters, including the heavy quark masses, from the moments and to employ them in the OPE expression for the total width. A determination of  $|V_{cb}|$  follows from the comparison with the experimental total rate.

The main ingredients for an accurate analysis of the experimental data have been known for some time. Two implementations are currently employed by the Heavy Flavour Averaging Group (HFAG) [3], based on either the kinetic scheme [4, 5, 6, 7] (see also [8] for an earlier fit) or the  $1S$  scheme [9]. They both include terms through  $O(\alpha_s^2\beta_0)$  [10] and  $O(1/m_b^3)$  [11] but they use different perturbative schemes and approximations, include a slightly different choice of experimental data, and estimate the theoretical uncertainty in two distinct ways. According to the latest global fits the two methods yield very close results for  $|V_{cb}|$  [12].

The reliability of the inclusive method rests on our ability to control the higher order contributions in the double series and to constrain quark-hadron duality violation, *i.e.* effects beyond the OPE. The calculation of higher order effects allows us to verify the convergence of the double series and to reduce and properly estimate the residual theoretical uncertainty. Duality violation effects [13] can be constrained *a posteriori*, by looking at whether the OPE predictions fit the experimental data. This in turn essentially depends on precise measurements and precise OPE predictions. As the experimental accuracy reached at the  $B$  factories is already better than the theoretical accuracy for all the measured moments, any effort to improve the latter is strongly motivated.

There has been recent progress in this direction. First, the complete two-loop perturbative corrections to the width and to the moments of the lepton energy and hadronic mass distributions have been computed in Refs. [14, 15, 16]. This represents an important improvement with respect to the  $O(\alpha_s^2\beta_0)$  or BLM corrections, which in  $B$  decays generally dominate the  $O(\alpha_s^2)$  effects when  $\alpha_s$  is normalized at  $m_b$ . The main goal of this paper is to incorporate the new *non-BLM* corrections in the calculation of the semileptonic moments and to discuss their numerical impact in different schemes.

Higher order power corrections have also been recently considered: a first analysis of  $O(1/m_b^4)$  and  $O(1/m_Q^5)$  effects has been presented in [17]. In the higher orders of the OPE there is a proliferation of operators and therefore of non-perturbative parameters: as many as nine new expectation values appear at  $O(1/m_b^4)$ . Since they cannot be fitted from experi-

ment, the authors of Ref. [17] estimated them in the ground state saturation approximation and found a relatively small +0.4% effect on  $|V_{cb}|$ . While this sets the scale of higher order power corrections, it is for the moment unclear how much the result depends on the use of that approximation.

Another important source of theoretical uncertainty are the  $O(\alpha_s \Lambda_{\text{QCD}}^2/m_b^2)$  corrections to the width and to the moments. Only the  $O(\alpha_s \mu_\pi^2/m_b^2)$  terms are known [18] at present. A complete calculation of these effects has been recently performed in the case of inclusive radiative decays [19], where the  $O(\alpha_s)$  correction increase the coefficient of  $\mu_G^2$  in the rate by almost 20%. The extension of this calculation to the semileptonic case is in progress.

Inclusive semileptonic  $B$  decays are not only useful for the extraction of  $V_{cb}$ : the moments are sensitive to the values of the heavy quark masses and in particular to a linear combination of  $m_c$  and  $m_b$  [20], which to good approximation is the one needed for the extraction of  $|V_{cb}|$  [12]. The  $b$  quark mass and the OPE expectation values obtained from the moments are crucial inputs in the determination of  $|V_{ub}|$  from inclusive semileptonic decays, see *e.g.* [21] and refs. therein. The heavy quark masses and the OPE parameters are also relevant for a precise calculation of other inclusive decays like  $B \rightarrow X_s \gamma$  [22]. On the other hand,  $m_c$  and  $m_b$  can now be measured precisely from data on charm and bottom production in  $e^+e^-$  annihilation [23, 24], and from the moments of heavy quark current correlators computed on the lattice [25]. After checking the consistency of the constraints on  $m_{c,b}$  from semileptonic moments with these precise determinations, we should therefore include them as external inputs in the semileptonic fits (see [12] for a first attempt), eventually improving the accuracy of the  $|V_{ub}|$  and  $|V_{cb}|$  determinations.

In this paper we set up the tools for such improved analyses, extending the code developed in [6] and employed by HFAG to allow for NNLO fits in arbitrary mass schemes. In particular, in order to avoid the non-negligible uncertainty in the conversion from the kinetic scheme to  $\overline{\text{MS}}$  masses, we directly employ an  $\overline{\text{MS}}$  definition for the charm quark mass. In addition, the study of scheme and scale dependence gives us useful elements for an evaluation of the residual theoretical uncertainty.

It is worth recalling that in the current semileptonic fits the sensitivity to  $m_b$  and  $\mu_\pi^2$  is enhanced by the inclusion of the first two moments of the photon energy distribution in  $B \rightarrow X_s \gamma$ , which are now measured with good precision. Their impact on the fits is equivalent to that of a loose constraint on  $m_b$  with 80MeV uncertainty. However, the lower cut on the photon energy introduces a sensitivity to the Fermi motion of the  $b$ -quark inside the  $B$  meson [7] and there are poorly known subdominant contributions not described by the OPE even in the absence of a photon energy cut [26]. All this makes radiative moments different from semileptonic ones: in the following we will concentrate on the latter.

The paper is organized as follows: in the next Section we discuss the perturbative corrections of the lepton energy moments and the implementation of the NNLO contributions and we give tables of results in a few typical cases. In Section 3 we do the same for the moments of the invariant hadronic mass distribution. In Section 4 we review the relation between kinetic and  $\overline{\text{MS}}$  heavy quark definitions and provide numerical conversion formulas with uncertainty. Section 5 briefly summarizes the main results of the paper, while the

Appendix updates the prediction of the total rate of  $B \rightarrow X_c \ell \nu$  and gives an approximate formula for the extraction of  $|V_{cb}|$ .

## 2 Lepton energy moments at NNLO

In this section we consider the first few moments of the charged lepton energy spectrum in inclusive  $b \rightarrow c \ell \nu$  decays. They are experimentally measured with high precision (better than 0.2% in the case of the first moment) but at the  $B$ -factories a lower cut on the lepton energy,  $E_\ell \geq E_{cut}$ , is applied to suppress the background. In fact, experiments measure the moments at different values of  $E_{cut}$ . The relevant quantities are therefore

$$\langle E_\ell^n \rangle_{E_\ell > E_{cut}} = \frac{\int_{E_{cut}}^{E_{max}} dE_\ell E_\ell^n \frac{d\Gamma}{dE_\ell}}{\int_{E_{cut}}^{E_{max}} dE_\ell \frac{d\Gamma}{dE_\ell}}, \quad (1)$$

for  $n$  up to 3, as well as the ratio  $R^*$  between the rate with and without a cut

$$R^* = \frac{\int_{E_{cut}}^{E_{max}} dE_\ell \frac{d\Gamma}{dE_\ell}}{\int_0^{E_{max}} dE_\ell \frac{d\Gamma}{dE_\ell}}, \quad (2)$$

which is needed to relate the actual measurement of the rate with a cut to the total rate, from which one conventionally extracts  $V_{cb}$ . Since the physical information that can be extracted from the first three linear moments is highly correlated, it is convenient to study the central moments, namely the variance and asymmetry of the lepton energy distribution. In the following we will consider only  $R^*$  and

$$\ell_1 = \langle E_\ell \rangle_{E_\ell > E_{cut}}, \quad \ell_{2,3} = \langle (E_\ell - \langle E_\ell \rangle)^{2,3} \rangle_{E_\ell > E_{cut}}. \quad (3)$$

These four observables are all functions of  $m_b$  and of the two dimensionless quantities

$$r = \frac{m_c}{m_b}, \quad \xi = \frac{2E_{cut}}{m_b}. \quad (4)$$

Our calculation follows closely the one described in [6]. Apart from the inclusion of the complete  $O(\alpha_s^2)$  corrections there are a few changes and improvements worth mentioning: *i*) the complete  $O(\alpha_s)$  and  $O(\alpha_s^2 \beta_0)$  corrections to the charged leptonic spectrum have been first calculated in [27] and [28]. While they can be computed numerically for any value of  $\xi$  and  $r$ , a numerical integration would slow down the fitting routines significantly, hence the need for interpolation formulas that must be accurate in a wide range of  $\xi$  and  $r$  values, keeping in mind that the values of  $m_{c,b}$  may differ considerably from one scheme to another. The accuracy of the interpolation formulas is important because of the cancellations that will be discussed shortly and has been improved wrt [6] using high precision numerical results based on [10]. The approximations used for the  $O(\alpha_s)$  and  $O(\alpha_s^2 \beta_0)$  corrections to the linear moments are now quite precise and their range extends to  $0 < \xi < 0.75$  and  $0.18 < r < 0.28$ ;

*ii*) the code can now be used in the kinetic scheme at arbitrary values of the infrared cutoff  $\mu$  and with other definition of the quark masses and of the expectation values. In particular the  $\overline{\text{MS}}$  definition of  $m_c$  is now implemented; *iii*) in the kinetic scheme we now normalize the matrix element of the Darwin operator,  $\rho_D^3$ , at the same scale  $\mu$  as the quark masses and the other expectation values (in [6] it was normalized at  $\mu = 0$ ); *iv*) the code now computes the ratio  $R^*$ , defined in (2) and necessary to extrapolate the rate measured at the B factories to the total semileptonic width. Most of these changes have already been included in the version of the Fortran code employed by HFAG [3] in the last few years.

The  $O(\alpha_s^2)$  corrections that are not enhanced by  $\beta_0$  — we will call them *non-BLM corrections* — are known to be subdominant when  $\alpha_s$  is normalized at  $m_b$ . They have been recently computed in [14, 16, 15]. While Refs. [14, 16] adopt numerical methods and can take into account arbitrary cuts on the lepton energy, the authors of [15] expand the moments in powers of  $m_c/m_b$  and provide only results without cuts. The two calculations are in good agreement and their implementation in our codes is in principle straightforward. However, the strong cancellations occurring in the calculation of normalized central moments require a high level of numerical precision. Indeed, radiative corrections to the  $E_l$  spectrum tend to renormalize the tree level spectrum in a nearly constant way, i.e. hard gluon emission is comparatively suppressed. This implies that the perturbative corrections tend to drop out of normalized moments. Let us consider for instance the first leptonic moment in the kinetic scheme with  $\mu = 1$  GeV, using  $r = 0.25$ ,  $m_b = 4.6$  GeV and  $E_{cut} = 1$  GeV:

$$\begin{aligned} \langle E_l \rangle_{E_l > 1 \text{ GeV}} &= 1.54 \text{ GeV} \left[ 1 + (0.96_{den} - 0.93) \frac{\alpha_s}{\pi} + (0.48_{den} - 0.46) \beta_0 \left( \frac{\alpha_s}{\pi} \right)^2 \right. \\ &\quad \left. + [1.69(7) - 1.75(9)_{den}] \left( \frac{\alpha_s}{\pi} \right)^2 + O(1/m_b^2, \alpha_s^3) \right] \end{aligned} \quad (5)$$

It is interesting to note that such *kinematic* cancellations between numerator and denominator (identified by the subscript *den*) affect the  $O(\alpha_s)$ ,  $O(\alpha_s^2 \beta_0)$ , and two-loop non-BLM corrections in a similar way. We have indicated in brackets the numerical uncertainty of the non-BLM correction [14]: the resulting coefficient in that case is  $-0.06 \pm 0.12$ . Similar conclusions can be drawn at different values of the cut and for higher linear moments. As discussed in [16], these cancellations are not accidental. In the limit  $\xi \rightarrow \xi_{max} = 1 - r^2$  the cancellations between numerator and denominator are complete at any perturbative order: therefore the higher the cut, the stronger the cancellation. Moreover the peak of the lepton energy distribution is relatively narrow and close to the endpoint, which further protects the moments from radiative corrections.

In the case of the higher central moments, additional cancellations occur at each perturbative order between normalized moments. In  $\ell_2$ , for instance,  $\langle E_l^2 \rangle$  and  $\langle E_l \rangle^2$  tend to cancel each other: for the same inputs as in Eq.(6) we have

$$\ell_2 = \langle E_\ell^2 \rangle - \langle E_\ell \rangle^2 = (2.479 - 2.393) \text{ GeV}^2 = 0.087 \text{ GeV}^2.$$

Such cancellations are quite general and are further enhanced by higher  $E_{cut}$ . They are

simply a consequence of the fact that, as we have just seen, at each perturbative order the spectrum follows approximately the tree-level spectrum, which is peaked at  $\xi \approx 0.7 - 0.8$ .

One obvious consequence of the cancellations we have just discussed is that the numerical accuracy with which the non-BLM corrections are known becomes an issue. While the origin of the cancellations is understood, we need a precise calculation to know their exact extent, and the result will have some impact on the estimate of the remaining theoretical uncertainty.

The building blocks of the perturbative calculation are the adimensional moments

$$L_n = \frac{1}{\Gamma_0} \frac{1}{m_b^n} \int_{E_{cut}}^{E_{max}} dE_\ell E_\ell^n \frac{d\Gamma}{dE_\ell} \quad (6)$$

where  $\Gamma_0$  is the total width at the tree-level. Any  $L_n$  can be expanded in  $\alpha_s$  and  $1/m_b$

$$L_n = L_n^{(0)} + \frac{\alpha_s(m_b)}{\pi} L_n^{(1)} + \left(\frac{\alpha_s}{\pi}\right)^2 (\beta_0 L_n^{(\text{BLM})} + L_n^{(2)}) + L_n^{(\text{pow})} + \dots$$

where we have distinguished between BLM and non-BLM two-loop corrections ( $\beta_0 = 11 - \frac{2}{3}n_l$ ) and indicated by  $L_n^{(\text{pow})}$  the power-suppressed contributions. The expansion for the normalized moments is

$$\langle E_\ell^n \rangle = \frac{L_n^{(0)}}{L_0^{(0)}} \left[ 1 + \frac{\alpha_s(m_b)}{\pi} \eta_n^{(1)} + \left(\frac{\alpha_s}{\pi}\right)^2 \left( \beta_0 \eta_n^{(\text{BLM})} + \eta_n^{(2)} - \eta_n^{(1)} \frac{L_0^{(1)}}{L_0^{(0)}} \right) + \eta_n^{(\text{pow})} + \dots \right], \quad (7)$$

where

$$\eta_i^{(a)} = \frac{L_i^{(a)}}{L_i^{(0)}} - \frac{L_0^{(a)}}{L_0^{(0)}}, \quad (8)$$

and an analogous formula holds for  $R^*$ .

Both available non-BLM calculations have been performed in the on-shell scheme and give us results for  $L_n^{(2)}$  at different values of  $r$  with an uncertainty due either to the numerical integration (and therefore of statistical origin) or to the truncation of the  $r$  expansion. However,  $L_n^{(2)}$  has been computed at  $\xi \neq 0$  only numerically [16]. The two calculations can be combined in order to reduce the final uncertainty. In the analytic calculation of [15] the expansion of the  $O(\alpha_s^2)$  corrections to the moments at  $\xi = 0$  includes at most  $O(r^7)$  terms and converges quite slowly for  $r \sim 0.2 - 0.25$ , in the relevant physical range. We can take the size of the last term included,  $O(r^7)$ , as a rough estimate of its non-gaussian uncertainty. It turns then out that the combinations of two-loop non-BLM integrals  $L_i^{(2)}$  that enter the normalized moments,  $\eta_i^{(2)}$ , at  $\xi = 0$  and  $r \lesssim 0.26$  can be more accurately determined using [15] than using the tables of [16].

It is also helpful to notice that, since the electron energy spectrum must vanish at low energies at least like  $E_\ell^2$ , only terms  $O(\xi^3)$  and higher are relevant: the two-loop corrections  $\eta_i^{(2)}$  must be flat for small  $\xi$  and the results of [16] are perfectly consistent with this requirement. One can therefore perform a fit to all the available results at different  $r$  and  $\xi$  values using simple functions of  $\xi$  and  $r$ . We have checked that, given the level of accuracy provided in

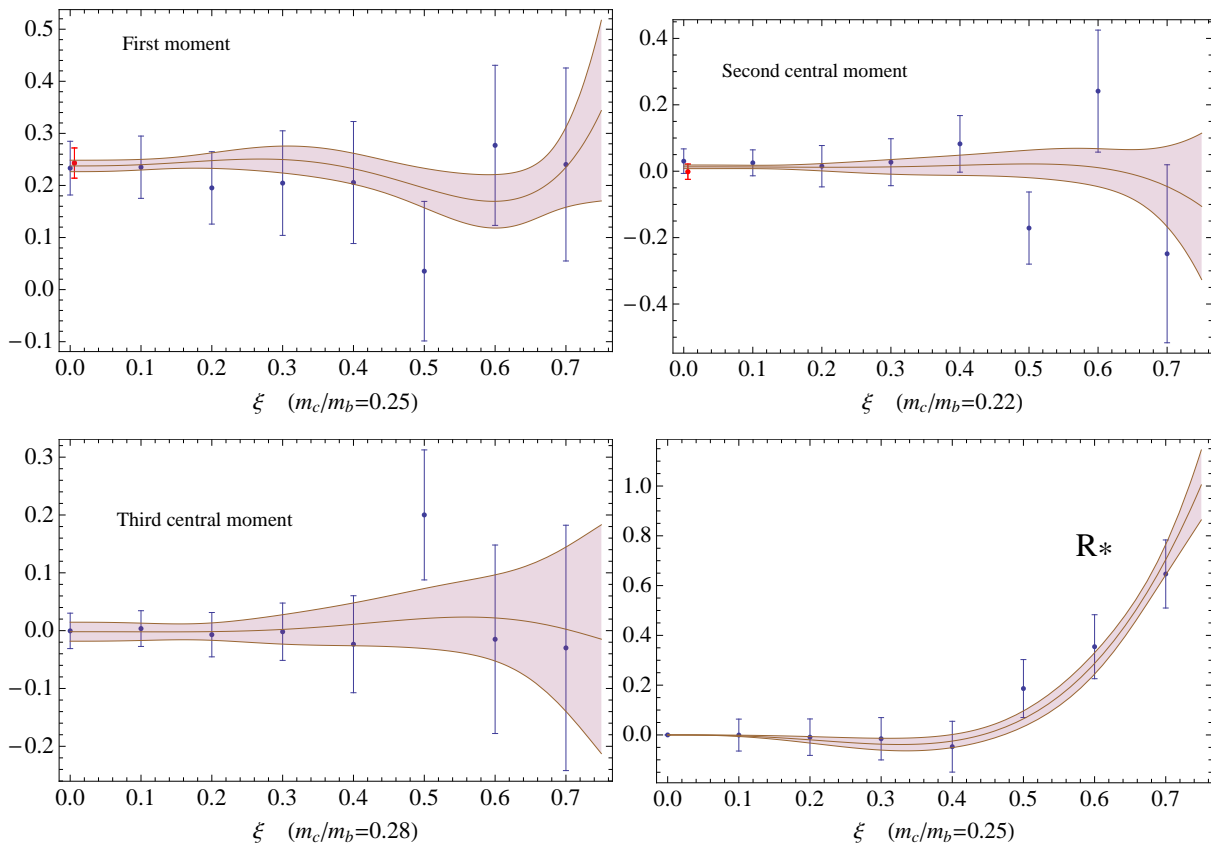


Figure 1: Combinations of two-loop non-BLM contributions entering the normalized central leptonic moments and  $R^*$ : numerical evaluation [16] with blue errors and analytic one [15] at  $\xi = 0$  with red errors vs. fits (shaded bands).

[16], it is sufficient to consider an expansion up to  $O(\xi^5)$  with coefficients linearly dependent on  $r$ . The  $\chi^2/dof$  is generally low, about 0.4, as the spread of central values in the low- $\xi$  region is much smaller than the size of the errors. We also know that the functions  $\eta_i^{(2)}(\xi, r)$  must vanish linearly at the endpoint  $\xi = 1 - r^2$ , and one can implement this constraint in the fit, but the result are unchanged for  $\xi < 0.7$ .

In the first plot in Fig. 1 we show the combination  $\eta_1^{(2)}$  that enters the first normalized leptonic moment  $\ell_1$  as a function of  $\xi$  for  $r = 0.25$ . In the plot we compare the numerical evaluations given in Table 1 of [16] and their associated error bars with the fit. At  $\xi = 0$  we also show the result of [15], whose uncertainty is estimated as explained above. The shaded band represents the  $1\sigma$  uncertainty of the fit. In the case of Eq. (6) the error of the non-BLM  $O(\alpha_s^2)$  coefficient estimated in this way is  $\pm 0.03$ , with a sizable reduction wrt that equation. For higher cuts and for values of  $r$  at the edge of the range  $0.2 \leq r \leq 0.28$  considered in [16] the reduction is weaker. In Fig. 2 we show the  $r$ -dependence of  $\eta_1^{(2)}(\xi = 0)$ , comparing the fit with the existing results. It is clear that a linear fit is perfectly adequate. The errors



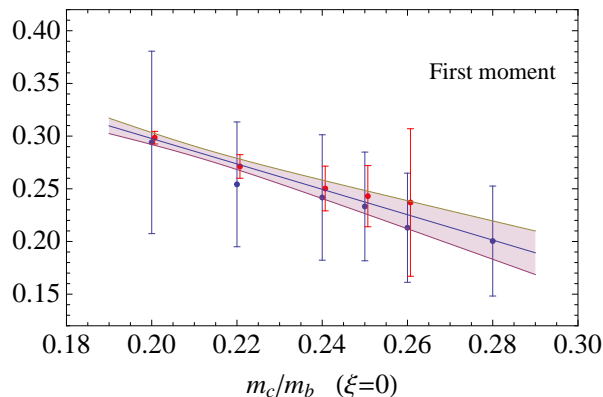


Figure 2: The non-BLM contribution  $\eta_1^{(2)}(\xi = 0)$  to the first leptonic moment as a function of  $r$ : numerical evaluation [16] with blue errors and analytic one [15] at  $\xi = 0$  with red errors vs. fits (shaded bands).

obtained by combining in quadrature the numerical uncertainties of  $L_1^{(2)}$  and  $L_0^{(2)}$  appear overestimated. We have found similar results for the higher linear moments, but we show in Fig.1 only the combinations that actually enter the second and third central moments,

$$\begin{aligned}\eta_{2c}^{(2)} &= w_2 \eta_2^{(2)} - 2 w_1^2 \eta_1^{(2)} \\ \eta_{3c}^{(2)} &= w_3 \eta_3^{(2)} + 3 w_1 (2 w_1^2 - w_2) \eta_1^{(2)} - 3 w_1 w_2 \eta_2^{(2)},\end{aligned}$$

where  $w_i = L_i^{(0)}/L_0^{(0)}$  are tree-level functions. Despite the residual uncertainty, the new results confirm that the pattern of cancellations observed at  $O(\alpha_s)$  and  $O(\alpha_s^2 \beta_0)$  carries on at the complete  $O(\alpha_s^2)$ . This is illustrated in Tables 1 and 2 for  $E_{cut} = 0$  and 1 GeV. In these Tables we report the values of the first three central moments for the reference values of the input parameters

$$\begin{aligned}m_b = 4.6 \text{ GeV}, \quad m_c = 1.15 \text{ GeV}, \quad \mu_\pi^2 = 0.4 \text{ GeV}^2, \quad \mu_G^2 = 0.35 \text{ GeV}^2 \\ \rho_D^3 = 0.2 \text{ GeV}^3, \quad \rho_{LS}^3 = -0.15 \text{ GeV}^3,\end{aligned}\tag{9}$$

and for  $\mu = 0$  (corresponding to the on-shell scheme) and  $\mu = 1 \text{ GeV}$ . The kinetic scheme expressions are obtained from the on-shell ones after re-expressing the pole quark masses and their analogues for  $\mu_\pi^2$  and  $\rho_D^3$  in terms of low energy running quantities, employing the two-loop contributions computed in [29] and re-expanding all perturbative series.<sup>1</sup>

In our calculation we remove all terms of  $O(\alpha_s \Lambda^2/m_b^2)$  because they are not yet known completely, but we retain suppressed terms of  $O(\alpha_s^2 \mu^3/m_b^3)$  that originate in the kinetic scheme from a simultaneous perturbative shift in  $m_b$  and  $\mu_\pi^2$  or  $\rho_D^3$ , although they turn out to be completely negligible in the case of leptonic moments.

<sup>1</sup>Unlike the  $O(\alpha_s^2)$  calculation of the moments, the kinetic scheme expressions of Ref. [29] do not explicitly

|                        | $\mu = 0$ |           |            | $\mu = 1\text{GeV}$ |           |            |
|------------------------|-----------|-----------|------------|---------------------|-----------|------------|
|                        | $\ell_1$  | $\ell_2$  | $\ell_3$   | $\ell_1$            | $\ell_2$  | $\ell_3$   |
| tree                   | 1.4131    | 0.1825    | -0.0408    | 1.4131              | 0.1825    | -0.0408    |
| $1/m_b^3$              | 1.3807    | 0.1808    | -0.0354    | 1.3807              | 0.1808    | -0.0354    |
| $O(\alpha_s)$          | 1.3790    | 0.1786    | -0.0354    | 1.3853              | 0.1811    | -0.0349    |
| $O(\beta_0\alpha_s^2)$ | 1.3731    | 0.1766    | -0.0350(1) | 1.3869              | 0.1820    | -0.0341(1) |
| $O(\alpha_s^2)$        | 1.3746(1) | 0.1767(2) | -0.0349(6) | 1.3865(1)           | 0.1816(2) | -0.0340(6) |
| tot error [6]          |           |           |            | 0.0125              | 0.0055    | 0.0026     |

Table 1: The first three leptonic moments for the reference values of the input parameters and  $E_{cut} = 0$ , in the on-shell and kinetic schemes. In parentheses the numerical uncertainty of the BLM and non-BLM contributions (see text).

|                        | $\ell_1$            | $\ell_2$  | $\ell_3$    | $R^*$     |
|------------------------|---------------------|-----------|-------------|-----------|
|                        |                     | $\mu = 0$ |             |           |
| tree                   | 1.5674              | 0.0864    | -0.0027     | 0.8148    |
| $1/m_b^3$              | 1.5426              | 0.0848    | -0.0010     | 0.8003    |
| $O(\alpha_s)$          | 1.5398              | 0.0835    | -0.0010     | 0.8009    |
| $O(\beta_0\alpha_s^2)$ | 1.5343              | 0.0818(1) | -0.0009(2)  | 0.7992    |
| $O(\alpha_s^2)$        | 1.5357(2)           | 0.0821(6) | -0.0011(16) | 0.7992(1) |
|                        | $\mu = 1\text{GeV}$ |           |             |           |
| $O(\alpha_s)$          | 1.5455              | 0.0858    | -0.0003     | 0.8029    |
| $O(\beta_0\alpha_s^2)$ | 1.5468              | 0.0868(1) | 0.0005(2)   | 0.8035    |
| $O(\alpha_s^2)$        | 1.5466(2)           | 0.0866    | 0.0002(16)  | 0.8028(1) |
| $O(\alpha_s^2)^{**}$   | –                   | 0.0865    | 0.0004      | –         |
| tot error [6]          | 0.0113              | 0.0051    | 0.0022      |           |

Table 2: The first three leptonic moments for the reference values of the input parameters and  $E_{cut} = 1\text{GeV}$ , in the on-shell and kinetic schemes.

|                        | $\mu = 1\text{GeV}, m_c^{\overline{\text{MS}}}(2\text{GeV})$ |           |             |           |
|------------------------|--|-----------|-------------|-----------|
|                        | $\ell_1$   | $\ell_2$  | $\ell_3$    | $R^*$     |
| tree                   | 1.5792   | 0.0890    | -0.0032     | 0.8200    |
| $1/m_b^3$              | 1.5536   | 0.0873    | -0.0013     | 0.8058    |
| $O(\alpha_s)$          | 1.5502   | 0.0869    | -0.0003     | 0.8056    |
| $O(\beta_0\alpha_s^2)$ | 1.5540   | 0.0884(1) | 0.0004(2)   | 0.8073    |
| $O(\alpha_s^2)$        | 1.5523(3)  | 0.0879(6) | -0.0002(16) | 0.8061(1) |
| $O(\alpha_s^2)^{**}$   | –  | 0.0878    | 0.0004      | –         |
|                        | $\mu = 1\text{GeV}, m_c^{\overline{\text{MS}}}(3\text{GeV})$ |           |             |           |
|                        | $\ell_1$   | $\ell_2$  | $\ell_3$    | $R^*$     |
| tree                   | 1.6021   | 0.0940    | -0.0043     | 0.8296    |
| $1/m_b^3$              | 1.5748   | 0.0922    | -0.0020     | 0.8159    |
| $O(\alpha_s)$          | 1.5613   | 0.0894    | -0.0004     | 0.8118    |
| $O(\beta_0\alpha_s^2)$ | 1.5629   | 0.0904(1) | 0.0004(2)   | 0.8125    |
| $O(\alpha_s^2)$        | 1.5571(4)  | 0.0890(9) | -0.0008(25) | 0.8090(2) |
| $O(\alpha_s^2)^{**}$   | –  | 0.0889    | 0.0006      | –         |

Table 3: The first three leptonic moments for the reference values of the input parameters and  $E_{cut} = 1\text{GeV}$ , in the kinetic scheme with  $\overline{\text{MS}}$  charm mass evaluated at  $\mu = 2$  and  $3\text{GeV}$ , with  $m_c(2\text{GeV}) = 1.1\text{GeV}$  and  $m_c(3\text{GeV}) = 1\text{GeV}$ . The uncertainty in the  $O(\alpha_s^2)$  is larger in the second case because the  $m_c/m_b$  value is closer to the edge of the range considered in [16].

Non-BLM contributions to the leptonic moments are generally tiny in the kinetic scheme. This is not necessarily the case if we adopt other renormalization schemes. We illustrate the point by using an  $\overline{\text{MS}}$  definition of the charm quark mass. As mentioned in the Introduction, this may be useful for the inclusion in semileptonic fits of precise mass constraints. Table 3 shows the results at  $E_{cut} = 1\text{GeV}$  in the case the charm quark mass is renormalized in the  $\overline{\text{MS}}$  scheme at two different values of the  $\overline{\text{MS}}$  scale;  $\bar{\mu} = 2$  and  $3\text{GeV}$ . The bottom mass and the OPE parameters are still defined in the kinetic scheme. We observe that in this case the non-BLM corrections are not always negligible, especially at  $\bar{\mu} = 3\text{GeV}$ . This is due to the fact that the  $\overline{\text{MS}}$  running is numerically important and driven by non-BLM effects. The sizable non-BLM corrections found in this case are therefore related to the change of scheme for  $m_c$  which is known with high accuracy.

To better understand what drives larger corrections in the  $\overline{\text{MS}}$  scheme, let us now consider  $\ell_{1,2,3}$  for  $E_{cut} = 1\text{GeV}$  and reference inputs. A shift in  $m_{b,c}$  induces in the central leptonic

---

include finite charm mass effects in the loops. This mismatch will be ignored in the following: it is effectively equivalent to a perturbative redefinition of our mass parameters and it is relevant only when we translate them to other schemes, see Section 4.

| $E_{cut}$ | $\frac{\eta_1^{(2)}}{\eta_1^{(BLM)}}$ | $\frac{\eta_2^{(2)}}{\eta_2^{(BLM)}}$ | $\frac{\eta_3^{(2)}}{\eta_3^{(BLM)}}$ | $\frac{\eta_{2c}^{(2)}}{\eta_{2c}^{(BLM)}}$ |
|-----------|---------------------------------------|---------------------------------------|---------------------------------------|---|
| 0         | -0.28(1)                              | -0.26(1)                              | -0.26(1)                              | -0.15(9)                                    |
| 0.6       | -0.32(3)                              | -0.29(1)                              | -0.28(1)                              | -0.14(19)                                   |
| 0.9       | -0.33(4)                              | -0.32(2)                              | -0.30(1)                              | -0.21(30)                                   |
| 1.2       | -0.30(6)                              | -0.32(3)                              | -0.30(2)                              | -0.36(62)                                   |
| 1.5       | -0.33(9)                              | -0.31(4)                              | -0.27(2)                              | +0.3(1.4)                                   |

Table 4: Ratio of non-BLM to BLM contributions to the leptonic moments at various  $E_{cut}$  values, in the on-shell scheme.

moments the shifts

$$\begin{aligned} \delta\ell_1 &= 0.325 \delta m_b - 0.237 \delta m_c, & \delta\ell_2 &= 0.094 \delta m_b - 0.058 \delta m_c, \\ \delta\ell_3 &= 0.009 \delta m_b - 0.010 \delta m_c, \end{aligned} \tag{10}$$

which vanish for  $\delta m_c/\delta m_b \approx 1.4$ , 1.6 and 0.9, respectively. Therefore, the leptonic central moments, and particularly the first two, give similar constraints in the  $(m_c, m_b)$  plane. In the case of a change of mass scheme, the bulk of the shift in the leptonic moments is given by the above  $\delta\ell_i$ , where  $\delta m_{c,b}$  represent the difference between the on-shell masses and the masses in the new scheme. In the kinetic scheme with  $\mu = 1$  GeV we have  $\delta m_c/\delta m_b \approx 1.2$  at  $O(\alpha_s^2)$ , which explains why the change of scheme does not spoil the cancellations in the perturbative corrections, as shown in Table 2. In other schemes and for different values of  $\mu$  the situation can be different, and indeed when we adopt the  $\overline{\text{MS}}$  scheme for  $m_c$  with  $\bar{\mu} = 3$  GeV (lower sector of Table 3) we observe slightly larger perturbative corrections. As our calculation is complete at NNLO, one could worry that higher orders in  $\delta m_{c,b}$  could spoil the cancellations that occur in the on-shell scheme and lead to an underestimate of higher order corrections. This appears to be unlikely, except for large  $\overline{\text{MS}}$  scales; even that unnatural case, however, would be under control, as the  $O(\alpha_s^3)$   $\bar{\mu}$  evolution is known.

While in the case of  $\ell_1$  and  $R^*$  the numerical accuracy is always adequate for the fits to experimental data, the poor direct knowledge of irreducible non-BLM corrections to the second and especially the third central moment suggests to adopt for them a different approach. We have already argued that the two-loop calculations confirm that the cancellations occurring at  $O(\alpha_s)$  and  $O(\alpha_s^2\beta_0)$  replicate at  $O(\alpha_s^2)$  as well. This is further illustrated by Table 4 where the ratio between the non-BLM and BLM contributions to  $\eta_{1,2,3}$  are shown and, as usual, the uncertainty is dominated by that of the non-BLM fits. The ratio of non-BLM to BLM contributions is well determined and close to  $-0.3$ , but in the case of  $\eta_{2c}^{(2)}$  the uncertainty is much larger, especially at large cuts, namely where the cancellations are necessarily enhanced. We therefore choose to assume a value  $-0.2 \pm 0.1$  for this ratio and adopt it as default. In the case of  $\eta_{3c}^{(2)}$  the uncertainty is so much bigger than the effect that we simply remove this contribution, retaining however reducible non-BLM contributions that are important in the  $\overline{\text{MS}}$  scheme. Reference values for this default choice are reported in Tables 2, 3 in the row denoted by \*\*.

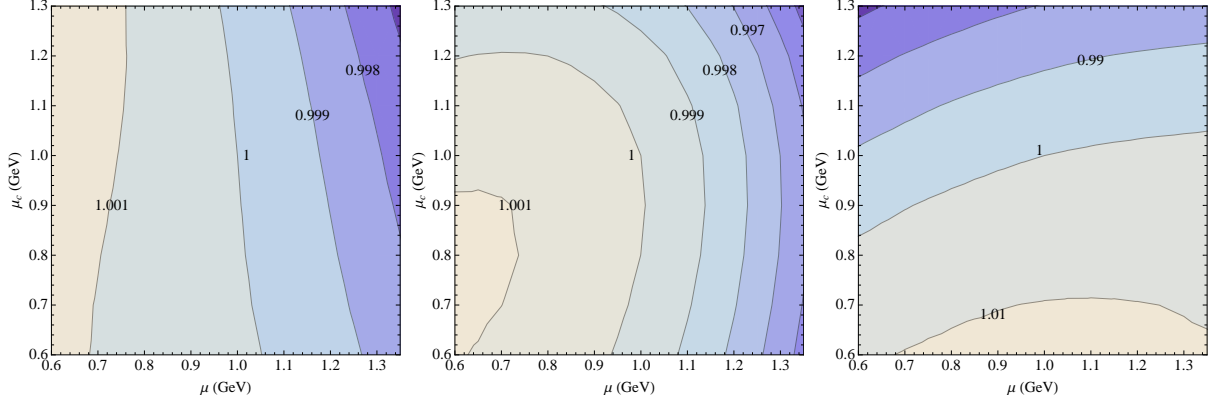


Figure 3:  $\mu$  and  $\mu_c$  dependence of the first three leptonic central moments at  $E_{cut} = 0$  normalized to their reference value  $\mu = \mu_c = 1$  GeV. The three plots refer to  $\ell_{1,2,3}$ , respectively.

## 2.1 Scale dependence of leptonic moments

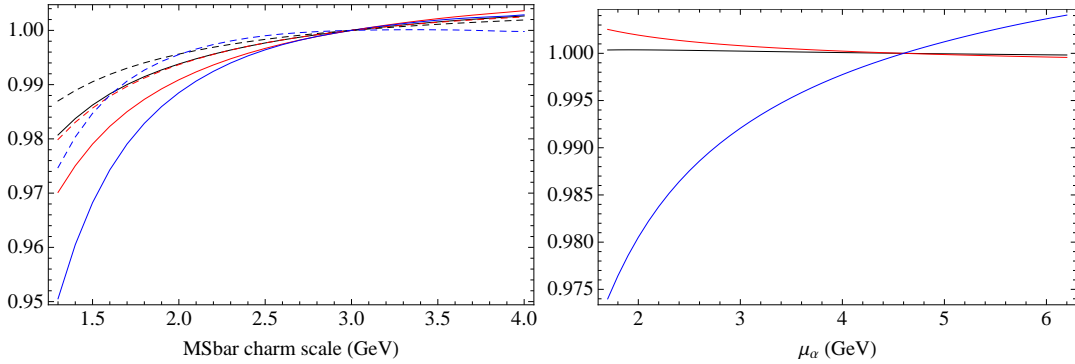


Figure 4: Dependence of the first three leptonic central moments at  $E_{cut} = 0$  on a) the charm  $\overline{\text{MS}}$  scale  $\bar{\mu}$  (left panel) and b) the scale of  $\alpha_s$  when the kinetic scheme is applied to  $m_c$  as well (right panel). The moments are normalized to their values at  $\bar{\mu} = 3$  GeV and  $\mu_\alpha = m_b$ , respectively. The kinetic cutoff is fixed at 1 GeV. The black, red, blue lines refer to  $\ell_{1,2,3}$ . The solid (dashed) lines refer to four (two) loop evolution.

The size of uncalculated higher order perturbative corrections can be estimated in various ways. We have already made a few remarks in this direction and we have studied the size of the NNLO contributions in various mass schemes. Now we study how our predictions for the leptonic moments depend on various unphysical scales that enter the calculation. In Fig. 3 we show the dependence of the leptonic moments in the kinetic scheme on the cutoff  $\mu$  and on  $\mu_c$ , the cutoff related to the kinetic definition of the charm mass. Indeed, there is no reason of principle to set  $\mu_c = \mu$  as we have done above. In the plots we have taken

the  $\mu = \mu_c = 1 \text{ GeV}$  values of the  $b$  and  $c$  masses and of the OPE parameters  $\mu_\pi^2$  and  $\rho_D^3$  in Eq. (9) and have evolved them to different  $\mu, \mu_c$  using  $O(\alpha_s^2)$  perturbative expansions [29] with  $\alpha_s(m_b)$ . The plots refer to  $E_{cut} = 0$ , but the absolute size of the scale dependence is similar at different cuts, while the relative size varies in an obvious way. Notice that for values of  $\mu$  significantly higher than 1 GeV the kinetic definition may lead to artificially large perturbative corrections, especially in the case of the charm mass. In the acceptable range shown in the plots the scale dependence is small, and only for  $\ell_1$  it is larger than the whole  $O(\alpha_s^2)$  correction.

The plot on the left of Fig. 4 refers instead to the calculation with the charm mass defined in the  $\overline{\text{MS}}$ . It shows the dependence on the charm mass scale  $\bar{\mu}$  for fixed kinetic cutoff  $\mu = 1 \text{ GeV}$ , normalized to the values  $\bar{\mu} = 3 \text{ GeV}$ ,  $m_c(3 \text{ GeV}) = 1 \text{ GeV}$ . We have evolved  $\bar{m}_c$  using the four loop Renormalization Group Evolution (RGE) implemented in [30]. It is clear that in this case higher order corrections present in the four loop RGE (and to a lesser extent even in the two loop RGE, see Fig. 4) lead to very sizable corrections and that scales below 2 GeV should be avoided. Even above 2 GeV the observed scale dependence of  $\ell_1$  is larger than its whole perturbative contribution. This is not an indication of large higher order corrections in the calculation of the moments, but only in the  $\overline{\text{MS}}$  evolution of  $m_c$ . The best procedure to extract  $m_c$  is therefore to compute moments at a scale  $\bar{\mu} \approx 2 \text{ GeV}$  that tends to minimize the corrections to the moments, and then to evolve to other scales using the most accurate RGE formula.

Finally, in the right-hand plot of Fig. 4 we show the dependence of the kinetic scheme results on the  $\overline{\text{MS}}$  scale of  $\alpha_s, \mu_\alpha$ , for fixed cutoff  $\mu = \mu_c = 1 \text{ GeV}$ . The evolution of  $\alpha_s$  is again computed at 4 loops, using  $\alpha_s(m_b) = 0.22$  as input. Due to its direct connection with the size of the perturbative contributions, the  $\mu_\alpha$  dependence is generally tiny, with the only exception of  $\ell_3$ . For instance, using  $\alpha_s(m_b/2)$  instead of  $\alpha_s(m_b)$  in Table 1, we would have  $\ell_1 = 1.3870 \text{ GeV}$  in place of 1.3865 GeV.

We will briefly come back to the scheme dependence of the leptonic moments in Sec. 4. Before turning to the hadronic moments, however, it is useful to spend a few words on the estimate of the total theoretical uncertainty of the leptonic moments, a subject of great importance for the global fits from which we extract  $|V_{cb}|$ . In Ref. [6] and in the fits based on it, the overall theoretical uncertainty related to  $\ell_i$  was computed by adding in quadrature various contributions: the shifts in  $\ell_i$  due to a  $\pm 20\%$  ( $\pm 30\%$ ) variation in  $\mu_\pi^2$  and  $\mu_G^2$  ( $\rho_D^3$  and  $\rho_{LS}^3$ ), a  $\pm 20 \text{ MeV}$  variation in  $m_{c,b}$ , and a  $\pm 0.04$  variation in  $\alpha_s$ . The uncertainty estimated in this way is reported in the last row of Tables 1 and 2: in all cases it is about five times larger than the current experimental one. Following the inclusion of the NNLO calculation we can now slightly reduce this estimate. Keeping in mind the remaining sources of theoretical uncertainty<sup>2</sup>, one could use the same method with a  $\pm 10 \text{ MeV}$  variation in  $m_{c,b}$  and  $\pm 0.02$  in  $\alpha_s$ ; in this way the total theoretical uncertainty in  $\ell_1$  is reduced by  $\sim 25\%$  wrt the last row in Tables 1 and 2, while the improvement is only minor for  $\ell_{2,3}$ .

---

<sup>2</sup>While the  $O(\alpha_s \mu_\pi^2 / m_b^2)$  contributions to  $\ell_i$  are tiny [18], the  $O(1/m_b^{4,5})$  corrections estimated in Ref. [17] are almost as large as the total error in the last row of Tables 1 and 2.

### 3 Hadronic mass moments at NNLO

At the time Ref. [6] was published not even all the  $O(\alpha_s)$  corrections to the hadronic moments were available for  $\xi \neq 0$ , and therefore the original calculation in the kinetic scheme was rather incomplete. The original code underwent a subsequent upgrade to include the full  $O(\beta_0\alpha_s^2)$ , computed numerically following [10] and implemented through precise interpolation formulas, and in this form has been employed in recent HFAG analyses. Here we discuss the implementation of the complete NNLO corrections and present a few results. The code for the hadronic moments shares the same features of the leptonic code, including flexibility in the choice of the scheme and of all the relevant scales.

We recall that due to bound state effects the invariant mass  $M_X$  of the hadronic system, which is measured experimentally, is related to the invariant mass  $m_x$  and energy  $e_x$  of the partonic (quarks and gluons) final state by

$$M_X^2 = m_x^2 + 2e_x\bar{\Lambda} + \bar{\Lambda}^2, \quad (11)$$

where  $\bar{\Lambda} = M_B - m_b$ . Since  $\bar{\Lambda} \approx 0.7\text{GeV}$  is relatively large, we do not expand in  $\bar{\Lambda}/m_b$  and retain all powers of  $\bar{\Lambda}$ . It follows from Eq. (11) that the  $M_X^2$  moments are linear combinations of the moments of  $m_x^2$  and  $e_x$ , namely of the building blocks

$$M_{ij} = \frac{1}{\Gamma_0} \frac{1}{m_b^{2i+j}} \int_{E_\ell > E_{cut}} (m_x^2 - m_c^2)^i e_x^j d\Gamma. \quad (12)$$

For instance, in the case of the first normalized moment we have

$$\langle M_X^2 \rangle = m_c^2 + \bar{\Lambda}^2 + m_b^2 \frac{M_{10}}{M_{00}} + 2m_b\bar{\Lambda} \frac{M_{01}}{M_{00}}.$$

Like in the case of leptonic moments, we consider only central higher moments, and specifically

$$h_1 = \langle M_X^2 \rangle, \quad h_2 = \langle (M_X^2 - \langle M_X^2 \rangle)^2 \rangle, \quad h_3 = \langle (M_X^2 - \langle M_X^2 \rangle)^3 \rangle. \quad (13)$$

The calculation of  $h_{1,2,3}$  requires the knowledge of the building blocks  $M_{ij}$  with  $i+j \leq 1, 2, 3$ , respectively. They receive both perturbative and non-perturbative power-suppressed contributions:

$$M_{ij} = M_{ij}^{(0)} + \frac{\alpha_s(m_b)}{\pi} M_{ij}^{(1)} + \left(\frac{\alpha_s}{\pi}\right)^2 \left( \beta_0 M_{ij}^{(\text{BLM})} + M_{ij}^{(2)} \right) + M_{ij}^{(\text{pow})} + \dots \quad (14)$$

where the tree-level contributions  $M_{ij}^{(0)}$  vanish for  $i > 0$  and we have distinguished between BLM and non-BLM two-loop corrections ( $\beta_0 = 11 - \frac{2}{3}n_l$ ,  $n_l = 3$ ). Since we are interested in the *normalized* moments, we will be mostly concerned with the combinations

$$\chi_{ij}^{(a)} = \frac{M_{ij}^{(a)}}{M_{00}^{(0)}} - \frac{M_{00}^{(a)} M_{ij}^{(0)}}{(M_{00}^{(0)})^2}, \quad (15)$$

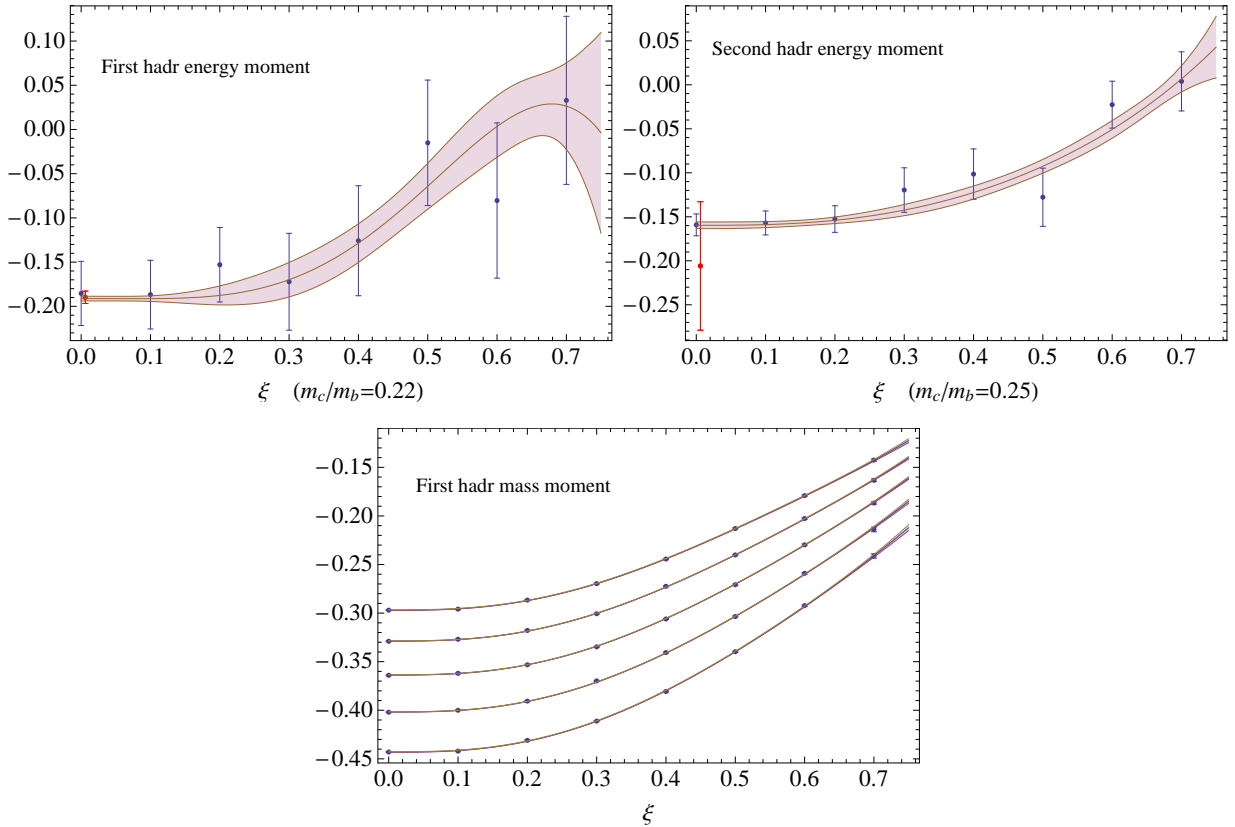


Figure 5: Combinations of two-loop non-BLM contributions  $\chi_{01}^{(2)}$ ,  $\chi_{02}^{(2)}$ , and  $\chi_{10}^{(2)}$  entering the hadronic moments: numerical evaluation [16] with blue errors and analytic one [15] at  $\xi = 0$  with red errors vs. fits (shaded bands).  $\chi_{10}^{(2)}$  (lower panel) is shown for  $r = 0.2, 0.22, 0.24, 0.26, 0.28$ .

with  $a = 1, \text{BLM}, 2, \text{pow}$ , which enter the perturbative and non-perturbative expansion for the normalized moments and are functions of  $\xi$  and  $r$ :

$$\frac{M_{ij}}{M_{00}} = \frac{M_{ij}^{(0)}}{M_{00}^{(0)}} + \frac{\alpha_s(m_b)}{\pi} \chi_{ij}^{(1)} + \left(\frac{\alpha_s}{\pi}\right)^2 \left( \beta_0 \chi_{ij}^{(\text{BLM})} + \chi_{ij}^{(2)} - \frac{M_{00}^{(1)}}{M_{00}^{(0)}} \chi_{ij}^{(1)} \right) + \chi_{ij}^{(\text{pow})} + \dots \quad (16)$$

The first  $O(\alpha_s)$  calculation appeared in [31] and was later completed in [32, 33, 10], while the  $O(\alpha_s^2 \beta_0)$  (BLM) calculation was presented in [33, 10]. Analytic expressions for the  $O(\alpha_s)$  contributions to the building blocks  $M_{ij}$  with  $i \neq 0$  are available as functions of  $\xi, r$  [10]. For the remaining building blocks and for all the  $O(\alpha_s^2 \beta_0)$  we employ high-precision two-parameters interpolation formulas to the results of the numerical code of Ref. [10], which are valid in the range  $0 < \xi < 0.8$  and  $0.18 < r < 0.29$ . The use of these approximations induces a negligible error.

The complete NNLO results presented here are based on the on-shell scheme results of Refs. [15, 16]. Ref. [15] provides us with NNLO contributions to the first two  $e_x$  moments



| $E_{cut}$ | $\frac{\chi_{01}^{(2)}}{\chi_{01}^{(2, \text{BLM})}}$ | $\frac{\chi_{10}^{(2)}}{\chi_{10}^{(2, \text{BLM})}}$ | $\frac{\chi_{02}^{(2)}}{\chi_{02}^{(2, \text{BLM})}}$ | $\frac{\chi_{11}^{(2)}}{\chi_{11}^{(2, \text{BLM})}}$ | $\frac{\chi_{12}^{(2)}}{\chi_{12}^{(2, \text{BLM})}}$ |
|-----------|---|---|---|---|---|
| 0         | -0.24(1)  | -0.24   | -0.23(1)  | -0.24   | -0.24   |
| 0.6       | -0.25(2)  | -0.24   | -0.24(1)  | -0.24   | -0.24   |
| 0.9       | -0.26(3)  | -0.23   | -0.24(1)  | -0.23   | -0.24   |
| 1.2       | -0.26(5)  | -0.23   | -0.24(2)  | -0.23   | -0.23   |
| 1.5       | -0.14(20)   | -0.23   | -0.17(7)  | -0.23   | -0.24   |

Table 5: Ratio of various perturbative contributions relevant to the hadronic moments at various  $E_{cut}$  values, in the on-shell scheme.

|                        | $\mu = 0$ |          |         | $\mu = 1\text{GeV}$ |          |         |
|------------------------|-----------|----------|---------|---------------------|----------|---------|
|                        | $h_1$     | $h_2$    | $h_3$   | $h_1$               | $h_2$    | $h_3$   |
| LO                     | 4.420     | 0.199    | -0.03   | 4.420               | 0.199    | -0.03   |
| power                  | 4.515     | 0.767    | 5.51    | 4.515               | 0.767    | 5.51    |
| $O(\alpha_s)$          | 4.662     | 1.239    | 7.78    | 4.504               | 1.069    | 6.13    |
| $O(\beta_0\alpha_s^2)$ | 4.834     | 1.661    | 9.51    | 4.493               | 1.301    | 6.39    |
| $O(\alpha_s^2)$        | 4.811     | 1.603(5) | 9.22(7) | 4.495               | 1.222(5) | 6.24(7) |
| tot error [6]          |           |          |         | 0.143               | 0.510    | 1.38    |

Table 6: The first three hadronic moments for the reference values of the input parameters and  $E_{cut} = 0$ , in the on-shell and kinetic schemes.

at  $\xi = 0$ , and we have the non-BLM contributions to several of the building blocks from Ref. [16]. In all the available cases we proceed in the same way as for leptonic moments and perform fits to the tables of [16] and to the  $\xi = 0$  of [15]; some of the results are shown in Fig. 5. Unfortunately not all the building blocks needed for the second and third  $M_X^2$  moments are reported in the tables of [16]: the missing building blocks are  $M_{20}^{(2)}$ ,  $M_{21}^{(2)}$ , and  $M_{30}^{(2)}$ , which have been computed only for  $r = 0.25$  and for  $\xi = 0$  and  $0.435$  [34].

In order to deal with these three cases we observe that in the on-shell scheme the ratio of non-BLM to BLM contributions to  $\chi_{ij}$  is always remarkably insensitive to the value of  $\xi$ , as shown in Table 5, and in fact much more insensitive than the analogous ratios to the tree-level or one-loop contributions. In particular, this ratio is known precisely for  $i \neq 0$  and varies by about  $\pm 0.01$  in the range  $0.2 < r < 0.28$ . In view of the other sources of theoretical errors, it is therefore sufficient to estimate the missing  $\chi_{20}^{(2)}$ ,  $\chi_{30}^{(2)}$ ,  $\chi_{21}^{(2)}$  using the values of their ratios in the two available points, and to assign them a  $\pm 0.02$  error:

$$\frac{\chi_{20}^{(2)}}{\chi_{20}^{(\text{BLM})}} = -0.215 \pm 0.020, \quad \frac{\chi_{21}^{(2)}}{\chi_{21}^{(\text{BLM})}} = -0.215 \pm 0.020, \quad \frac{\chi_{30}^{(2)}}{\chi_{30}^{(\text{BLM})}} = -0.205 \pm 0.020 \quad (17)$$

As illustrated in Fig. 5 by a few examples, the precision of the fits to the functions  $\chi_{0i}^{(2)}$  is similar to that of the functions  $\eta_i^{(2)}$  entering the leptonic moments. On the other

|                        | $\mu = 0$ |          |         | $\mu = 1\text{GeV}$ |          |         |
|------------------------|-----------|----------|---------|---------------------|----------|---------|
|                        | $h_1$     | $h_2$    | $h_3$   | $h_1$               | $h_2$    | $h_3$   |
| LO                     | 4.345     | 0.198    | -0.02   | 4.345               | 0.198    | -0.02   |
| $1/m_b^3$              | 4.452     | 0.515    | 4.90    | 4.452               | 0.515    | 4.90    |
| $O(\alpha_s)$          | 4.563     | 0.814    | 5.96    | 4.426               | 0.723    | 4.50    |
| $O(\beta_0\alpha_s^2)$ | 4.701     | 1.105    | 6.85    | 4.404               | 0.894    | 4.08    |
| $O(\alpha_s^2)$        | 4.682(1)  | 1.066(3) | 6.69(4) | 4.411(1)            | 0.832(4) | 4.08(4) |
| tot error [6]          |           |          |         | 0.149               | 0.501    | 1.20    |

Table 7: The first three hadronic moments for the reference values of the input parameters and  $E_{cut} = 1\text{GeV}$ , in the on-shell and kinetic schemes.

|                        | $\mu = 1\text{GeV}, m_c^{\overline{\text{MS}}}(2\text{GeV})$ |          |         | $\mu = 1\text{GeV}, m_c^{\overline{\text{MS}}}(3\text{GeV})$ |          |         |
|------------------------|--|----------|---------|--|----------|---------|
|                        | $h_1$  | $h_2$    | $h_3$   | $h_1$  | $h_2$    | $h_3$   |
| $1/m_b^3$              | 4.301  | 0.551    | 4.94    | 4.020  | 0.618    | 5.02    |
| $O(\alpha_s)$          | 4.355  | 0.758    | 4.60    | 4.192  | 0.830    | 4.79    |
| $O(\beta_0\alpha_s^2)$ | 4.304  | 0.936    | 4.21    | 4.169  | 1.015    | 4.49    |
| $O(\alpha_s^2)$        | 4.328  | 0.865(4) | 4.18(4) | 4.245(1)   | 0.922(5) | 4.38(4) |

Table 8: The first three hadronic moments for the reference values of the input parameters and  $E_{cut} = 1\text{GeV}$ , in the kinetic scheme with  $\overline{\text{MS}}$  charm mass evaluated at  $\mu = 2$  and  $3\text{GeV}$ , with  $m_c(2\text{GeV}) = 1.1\text{GeV}$  and  $m_c(3\text{GeV}) = 1\text{GeV}$ . The uncertainty in the  $O(\alpha_s^2)$  is larger in the second case because the  $m_c/m_b$  value is closer to the edge of the range considered in [16].

hand, the numerical evaluation of [16] is very accurate in the case of  $\chi_{ij}^{(2)}$  for  $i > 0$  and a quadratic dependence on  $r$  has to be included in the functional form. As the cancellations between different contributions are not as severe as for leptonic moments, the accuracy of the non-BLM corrections is in fact a minor issue in the case of hadronic moments.

Numerically, the non-BLM corrections in the on-shell scheme tend to partly compensate the BLM corrections and, as perturbative corrections in general, are more important than in the leptonic case, see Tables 6 and 7. The non-BLM effect is about 0.4%, 4%, 3% for  $h_{1,2,3}$ , respectively. In the kinetic scheme with  $\mu = 1\text{GeV}$  the non-BLM corrections to the first and third moment are slightly suppressed, while the non-BLM correction to  $h_2$  is larger than in the on-shell scheme (7-9%), see also Fig. 6. It is worth reminding that the perturbative contributions to the building blocks  $M_{11}$ ,  $M_{20}$  and  $M_{10}$  (all vanishing at tree-level) are dominant in  $h_2$ , and that these building blocks are known only at the next-to-leading order level. This explains the large relative value of the non-BLM corrections and implies a commensurate uncertainty. But the results shown in the Tables hide an important cancellation between the  $\mu_\pi^2$  and  $\rho_D^3$  contributions to  $h_2$  for the reference values of Eq. (9): for  $E_{cut} = 1\text{GeV}$  they are about  $+1.6$  and  $-1.2\text{GeV}^4$ , respectively. Non-perturbative contributions indeed dominate the higher moments  $h_{2,3}$ , which are therefore subject to much larger uncertainties from both

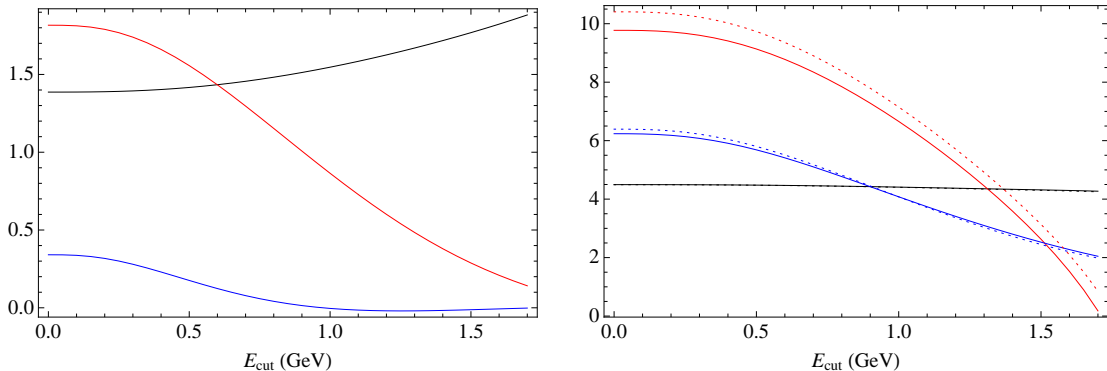


Figure 6:  $E_{cut}$  dependence of leptonic (left) and hadronic (right) at NNLO in the kinetic scheme with  $\mu = \mu_c = 1$  GeV. The black, red, blue lines refer to  $\ell_1$ ,  $10 \times \ell_2$ ,  $-10 \times \ell_3$  and to  $h_1$ ,  $8 \times h_2$ ,  $h_3$ , respectively, each expressed in GeV to the appropriate power. The dotted lines (indistinguishable for the leptonic moments) represent the predictions at  $O(\alpha_s^2 \beta_0)$ .

higher order terms in the OPE and the missing  $O(\alpha_s)$  corrections to the Wilson coefficients of the dimension 5 and 6 operators.

### 3.1 Scale dependence of hadronic moments

The  $\mu$  and  $\mu_c$  dependence of the hadronic moments in the kinetic scheme is shown in Fig. 7 for  $E_{cut} = 1$  GeV. The first moment has very small residual scale dependence, like the leptonic moments. Since the second and third hadronic moments receive much larger power and perturbative contributions, the larger  $\mu$  and especially  $\mu_c$  dependence is not surprising.

The results of the calculation of the moments when the charm mass is renormalized in the  $\overline{\text{MS}}$  scheme are illustrated in Table 8 for two different values of the charm scale  $\bar{\mu}$ . It is interesting that for  $\bar{\mu} = 3$  GeV the change of scheme induces large non-BLM corrections, suggesting that  $\bar{\mu} = 2$  GeV might be a better choice. Fig. 8 is the analogue of Fig. 4 for the hadronic moments. The plot on the left shows the dependence on the charm mass scale  $\bar{\mu}$ , when  $h_{1,2,3}$  are normalized to their values for  $\bar{\mu} = 3$  GeV,  $m_c(3 \text{ GeV}) = 1$  GeV. In this case the  $\bar{\mu}$  dependence is even larger than in the leptonic case, but again it should not be interpreted as indication of large higher order corrections in the calculation of the moments and one should preferably use values  $\bar{\mu}$  that minimize the corrections to the moments.

Like the leptonic moments, the first hadronic moment can be used to constrain the heavy quark masses. The higher hadronic moments are too sensitive to higher dimensional expectation values to play a role in this respect. At reference values of the inputs and for  $E_{cut} = 1$  GeV, a small shift in  $m_{b,c}$  induces

$$\delta h_1 = -4.84 \delta m_b + 3.08 \delta m_c,$$

which vanish for  $\delta m_c / \delta m_b \approx 1.6$ . Therefore,  $h_1$  gives a constraint in the  $(m_c, m_b)$  plane very

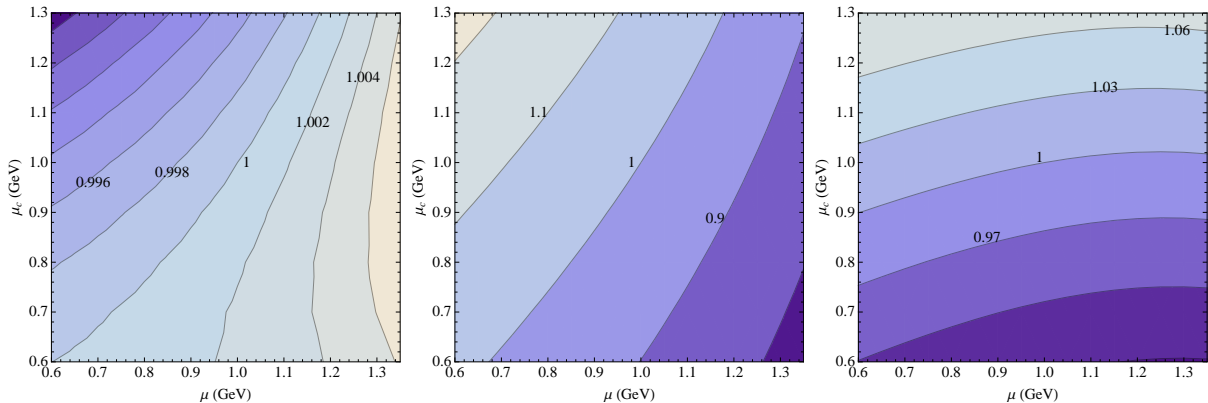


Figure 7:  $\mu$  and  $\mu_c$  dependence of the first three hadronic central moments at  $E_{cut} = 1$  GeV normalized to their reference value  $\mu = \mu_c = 1$  GeV. The three plots refer to  $h_{1,2,3}$ , respectively.

similar to the leptonic central moments. The considerations on scheme dependence made after Eq. (10) apply to the first hadronic moment as well.

Finally, in the right-hand plot of Fig. 8 we show the dependence of the kinetic scheme results on the  $\overline{\text{MS}}$  scale of  $\alpha_s$ ,  $\mu_\alpha$ , for fixed cutoff  $\mu = \mu_c = 1$  GeV. The evolution of  $\alpha_s$  is again computed at 4 loops, using  $\alpha_s(m_b) = 0.22$  as input. Due to its direct connection with the size of the perturbative contributions, the  $\mu_\alpha$  dependence is small for  $h_1$ . The strong residual dependence of  $h_2$ , on the other hand, suggests that in the absence of higher order corrections, it would be prudent to choose  $\mu_\alpha$  close to  $m_b/2$ .

The overall theoretical errors computed using the method proposed in [6] are reported in the last row of Tables 6 and 7: they are generally a factor two or more larger than the present experimental ones. Cutting by half the variation in  $m_{b,c}$  and  $\alpha_s$ , as it was proposed in the previous Section, leads to a 25-30% smaller total uncertainty on  $h_1$ , while the error on  $h_{2,3}$  is almost unaffected. The calculation of  $O(\alpha_s)$  corrections to the Wilson coefficients and that of higher orders in the OPE [17], will have a stronger impact on the total uncertainty. We also recall that the  $O(1/m_b^{4,5})$  contributions to  $h_i$  found in Ref. [17] are of the same order of magnitude of the total error in the last row of Tables 6 and 7, while those of  $O(\alpha_s \mu_\pi^2)$  [18] are comparatively small.

## 4 Mass scheme conversion

Semileptonic moments provide interesting constraints on the bottom and charm masses, which can be compared and combined with other experimental determinations of these parameters. Since in many applications the quark masses are renormalized in the  $\overline{\text{MS}}$ , we will now review the relation between the kinetic and  $\overline{\text{MS}}$  definitions of the heavy quark masses. Accurate conversion formulas can also be used to study the scheme dependence of our results. The perturbative relation between the quark pole mass and the kinetic mass is known

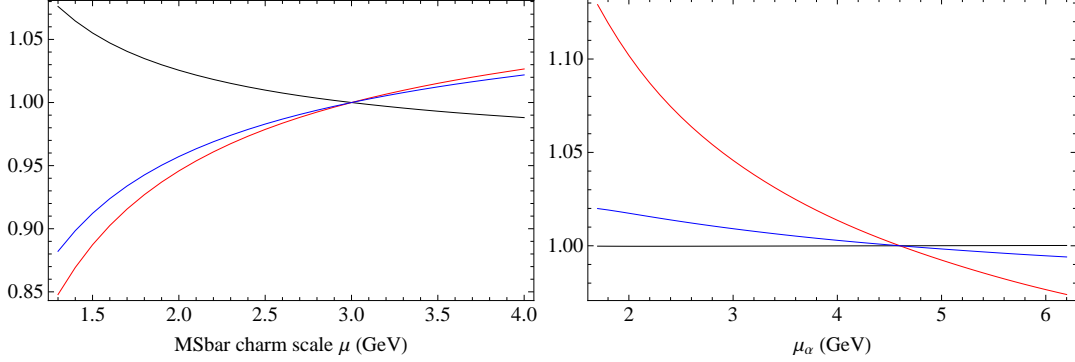


Figure 8: Dependence of  $h_{1,2,3}$  at  $E_{cut} = 0$  on *a*) the charm  $\overline{\text{MS}}$  scale  $\bar{\mu}$  (left panel) and *b*) the scale of  $\alpha_s$  when the kinetic scheme is applied to  $m_c$  as well (right panel). The moments are normalized to their values at  $\bar{\mu} = 3 \text{ GeV}$  and  $\mu_\alpha = m_b$ , respectively. The kinetic cutoff is fixed at 1 GeV. The black, red, blue lines refer to  $h_{1,2,3}$ .

completely at  $O(\alpha_s^2)$  and  $O(\alpha_s^3\beta_0^2)$  [29]. Combining it with the one between pole and  $\overline{\text{MS}}$  masses, known to  $O(\alpha_s^3)$  [35], one gets the following NNLO expansion for the ratio between the  $\overline{\text{MS}}$  mass  $\bar{m}(\bar{\mu})$  and its kinetic counterpart  $m(\mu)$

$$\begin{aligned}
\frac{\bar{m}(\bar{\mu})}{m(\mu)} &= 1 - \frac{4}{3} \frac{\alpha_s^{(n_l)}(M)}{\pi} \left( 1 - \frac{4}{3} \frac{\mu}{m(\mu)} - \frac{\mu^2}{2m(\mu)^2} + \frac{3}{4} L \right) \\
&+ \left( \frac{\alpha_s}{\pi} \right)^2 \left\{ \left[ -\frac{2}{3} L + \left( \frac{1}{3} \ln \frac{M}{2\mu} + \frac{13}{18} \right) \beta_0^{(n_l)} - \frac{\pi^2}{3} + \frac{47}{18} \right] \frac{\mu^2}{m^2} \right. \\
&+ \left[ -\frac{16}{9} L + \left( \frac{8}{9} \ln \frac{M}{2\mu} + \frac{64}{27} \right) \beta_0^{(n_l)} - \frac{8\pi^2}{9} + \frac{188}{27} \right] \frac{\mu}{m} - \frac{4}{3} \sum_i^{n_l} \Delta \left( \frac{m_i}{m} \right) \\
&+ \frac{7}{12} L^2 - \frac{2L}{9} - \left[ \frac{L^2}{8} + \frac{13L}{24} + \ln \frac{M^2}{\bar{\mu}^2} \left( \frac{L}{4} + \frac{1}{3} \right) + \frac{\pi^2}{12} + \frac{71}{96} \right] \beta_0^{(n_l)} \\
&\left. + \frac{\zeta(3)}{6} - \frac{\pi^2}{9} \ln 2 + \frac{7\pi^2}{12} - \frac{169}{72} + \left( \frac{2}{9} + \frac{L}{6} \right) \ln \frac{m_h^2}{\bar{\mu}^2} \right\}, \tag{18}
\end{aligned}$$

where we have used

$$L = \ln [\bar{\mu}^2/m(\mu)^2], \quad \beta_0^{(n_l)} = 11 - 2/3 n_l, \quad \Delta(x) = \frac{\pi^2}{8} x - 0.597x^2 + 0.230x^3.$$

The function  $\Delta(x)$  arises from the two-loop diagrams with a closed massive quark loop in the relation between pole and  $\overline{\text{MS}}$  mass [36, 30]. It represents the correction to the massless loop and is only relevant in the case of charm mass effects on the  $b$  mass. As mentioned in footnote 1, such effects are not included in the conversion to the kinetic scheme, which is performed assuming charm to be decoupled [29]<sup>3</sup>. There is also a dependence on  $m_h$ , the

<sup>3</sup>Finite charm mass  $O(\alpha_s^2)$  effects in the transition between pole and kinetic mass can in principle be computed from Eq. (11) of [29].

mass scale that defines the threshold between  $n_l$  and  $n_l + 1$  quark flavors, generally set equal to  $m$ . In the limit  $\mu \rightarrow 0$  the above formula relates the pole and the  $\overline{\text{MS}}$  masses.

When the scale of the  $\overline{\text{MS}}$  mass is equal to the  $\overline{\text{MS}}$  mass itself and the coupling constant is evaluated at the mass scale the above formula reduces to

$$\begin{aligned} \frac{\overline{m}(\overline{m})}{m(\mu)} = & 1 - \frac{4}{3} \frac{\alpha_s(m)}{\pi} \left( 1 - \frac{4}{3} \frac{\mu}{m(\mu)} - \frac{\mu^2}{2m(\mu)^2} \right) \\ & + \left( \frac{\alpha_s}{\pi} \right)^2 \left\{ \left[ \left( \frac{1}{3} \ln \frac{m}{2\mu} + \frac{13}{18} \right) \beta_0^{(n_l)} - \frac{\pi^2}{3} + \frac{23}{18} \right] \frac{\mu^2}{m^2} \right. \\ & + \left[ \left( \frac{8}{9} \ln \frac{m}{2\mu} + \frac{64}{27} \right) \beta_0^{(n_l)} - \frac{8\pi^2}{9} + \frac{92}{27} \right] \frac{\mu}{m} - \left( \frac{\pi^2}{12} + \frac{71}{96} \right) \beta_0^{(n_l)} \\ & \left. + \frac{\zeta(3)}{6} - \frac{\pi^2}{9} \ln 2 + \frac{7\pi^2}{12} + \frac{23}{72} - \frac{4}{3} \sum_i^{n_l} \Delta \left( \frac{m_i}{m} \right) \right\}. \end{aligned} \quad (19)$$

This result differs from those reported in [29, 5] by a term  $\left( \frac{\alpha_s}{\pi} \right)^2 \left( \frac{\pi^2}{18} + \frac{71}{144} \right)$ . The difference can be traced back to a mismatch between the number of quarks considered in the  $\overline{\text{MS}}$ -pole relation. In the limit  $\mu \rightarrow 0$ , Eq. (19) reproduces the standard two-loop  $\overline{\text{MS}}$ -pole relation, *cf.* Eq. 16 of [30] and [36]. The BLM corrections of  $O(\alpha_s^3 \beta_0^2)$  have been also considered in [29, 5].

## 4.1 Charm mass conversion

In the case of the charm mass we employ the two above formulas with  $n_l = 3$ , neglecting all  $\Delta$  functions. Eq. (19) with  $\alpha_s(m_c) = 0.41$  and  $m_c(1 \text{ GeV}) = 1.15$  gives

$$\overline{m}_c(\overline{m}_c) = 1.150 + 0.108\alpha_s + 0.071\alpha_s^2 = 1.329 \text{ GeV}, \quad (20)$$

where the one and two-loop contributions are identified by the subscript. Unsurprisingly, the perturbative series converges poorly. One easily verifies that BLM corrections dominate the two-loop contribution and that the result depends strongly on the scale of  $\alpha_s$ . The apparent convergence of the perturbative series can be drastically improved if one normalizes the charm mass at higher  $\overline{\text{MS}}$  scales. In fact, in the evolution of  $\overline{m}_c(\bar{\mu})$  to low scales the effect of RGE resummation becomes significant, but these contributions are absent from the fixed order NNLO calculation of the moments from which the kinetic mass could be extracted. In order to convert the results of a fit to the semileptonic moments in the kinetic scheme into the  $\overline{\text{MS}}$  scheme (or *vice versa*) it is therefore important to adopt a scale  $\bar{\mu}$  above 2 GeV. To illustrate the point let us use  $\bar{\mu} = 3 \text{ GeV}$  and adopt the central value of [23],  $\overline{m}_c(3 \text{ GeV}) = 0.986 \text{ GeV}$ . Inverting Eq. (18) and employing  $\alpha_s^{(3)}(3 \text{ GeV}) = 0.247$  (which corresponds to  $\alpha_s^{(4)}(m_b) = 0.22$  for  $m_b = 1.5 \text{ GeV}$ ), we obtain the kinetic charm mass

$$m_c^{\text{kin}}(1 \text{ GeV}) = 0.986 + 0.083\alpha_s + 0.022\alpha_s^2 = 1.091 \text{ GeV} \quad (21)$$

where the final result depends little on the scale of  $\alpha_s$  and on its exact value. The difference

$$m_c(1 \text{ GeV}) - \overline{m}_c(3\text{GeV}) = (0.105 \pm 0.015) \text{ GeV} \quad (22)$$

depends of course on the input  $\overline{m}_c(3\text{GeV})$ : for values between 0.95 and 1.05 GeV the central value moves from 0.096 to 0.121 GeV.

Using a lower scale  $\bar{\mu} = 2 \text{ GeV}$  the difference between kinetic and  $\overline{\text{MS}}$  is even smaller. Using  $\overline{m}_c(2\text{GeV}) = 1.092 \text{ GeV}$ , obtained from the four-loop evolution of the result of [23], one finds

$$m_c^{\text{kin}}(1\text{GeV}) = 1.092 + 0.037\alpha_s - 0.013\alpha_s^2 = 1.116 \text{ GeV} \quad (23)$$

with very small dependence on the scale of  $\alpha_s$ . The difference between the final results in Eqs. (21) and (23) is mostly due to our use of four-loop RGE to connect the inputs at  $\bar{\mu} = 3$  and 2 GeV. Our estimate is

$$m_c(1 \text{ GeV}) - \overline{m}_c(2\text{GeV}) = (0.024 \pm 0.010) \text{ GeV}, \quad (24)$$

whose central value varies between 0.017 and 0.032 GeV for  $\overline{m}_c(2\text{GeV})$  in the range 1.05 to 1.15 GeV. Eqs. (22,24) can be used to compare accurately the predictions for the semileptonic moments when the kinetic and  $\overline{\text{MS}}$  schemes are used for  $m_c$ . It turns out that the size of the scheme dependence found in this way is similar to the uncertainty due to scale dependence investigated in Secs. 2 and 3.

Once the relation between kinetic and  $\overline{\text{MS}}$  masses is known at large  $\bar{\mu}$  one can use the four-loop RGE together with Eq. (21,23) to compute  $\overline{m}_c(\overline{m}_c)$ . Using the more precise Eq. (23) we obtain

$$m_c(1 \text{ GeV}) - \overline{m}_c(\overline{m}_c) = 0.16 \pm 0.02 \text{ GeV}.$$

## 4.2 Bottom mass conversion

In the case of the relation between  $\overline{\text{MS}}$  and pole bottom mass the effects related to the charm mass in closed quark loops and described by  $\Delta(r)$  are small but not negligible. For realistic values of the charm to bottom mass ratio  $\Delta(r)$  compensates up to 40% of the light quark contribution, *i.e.* the term multiplied by  $n_l$  in the fourth line of Eq. (18). Since the corresponding effects are not included in the definition of kinetic  $m_b$ , in applying Eqs. (18,19) to the bottom mass we therefore have the following options

- (a) we decouple charm completely and set  $n_l = 3$ ,  $\Delta(r) = 0$ ;
- (b) we treat charm as massless and set  $n_l = 4$ ,  $\Delta(r) = 0$ ;
- (c) we decouple charm in the kinetic part of the calculation only, set  $n_l = 3$ , and replace  $\Delta(r) \rightarrow \Delta(r) - \frac{\pi^2}{24} - \frac{71}{192}$ .

It is clear that the correct result lies somewhere between (a) and (b). On the other hand, since the NNLO expressions of the semileptonic moments have been derived under the assumption

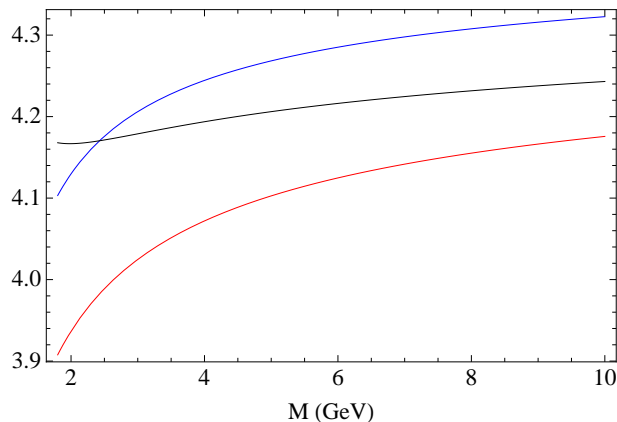


Figure 9:  $M$  dependence of  $m_b(m_b)$  in case (c) for  $m_b(1 \text{ GeV}) = 4.55 \text{ GeV}$ . The blue, red, black curves refer to one-loop, BLM, two-loop, respectively.

|                      | $\alpha_s(m_b)$ |       |       |
|----------------------|-----------------|-------|-------|
| $m_b(1 \text{ GeV})$ | 0.21            | 0.22  | 0.23  |
| 4.500                | 4.150           | 4.127 | 4.103 |
| 4.550                | 4.194           | 4.171 | 4.147 |
| 4.600                | 4.239           | 4.216 | 4.192 |

Table 9:  $\overline{m}_b(\overline{m}_b)$  for different values of the kinetic mass and of  $\alpha_s(m_b)$  in case (c) with  $M = 2.5 \text{ GeV}$ .

of charm decoupling in the relation between pole and kinetic masses, but we have otherwise kept the charm mass effects, option (c) is the most appropriate to convert the kinetic mass extracted from a NNLO fit to semileptonic moments into the  $\overline{\text{MS}}$  scheme.

Let us now illustrate the three options computing the  $\overline{\text{MS}}$  bottom mass from the kinetic one at a reference value  $\mu = 1 \text{ GeV}$ . We use  $m_b(1 \text{ GeV}) = 4.55 \text{ GeV}$  and  $\alpha_s(m_b) = 0.22$

$$\begin{aligned}
 \overline{m}_b(\overline{m}_b) &= 4.550 - 0.290_{\alpha_s} - 0.073_{\alpha_s^2} = 4.187 \text{ GeV}, & (a) \\
 &4.550 - 0.290_{\alpha_s} - 0.060_{\alpha_s^2} = 4.200 \text{ GeV}, & (b) \\
 &4.550 - 0.290_{\alpha_s} - 0.057_{\alpha_s^2} = 4.202 \text{ GeV}, & (c)
 \end{aligned}
 \tag{25}$$

from which we see that option (c) is numerically very close to (b). The BLM corrections are large in Eq. (25) but partly (50%) compensated by sizable non-BLM ones. The  $O(\alpha_s^3 \beta_0^2)$  corrections [29] shift  $\overline{m}_b(\overline{m}_b)$  further down by about 20 MeV. The dependence of the NNLO result on the scale of  $\alpha_s$  is shown in Fig. 9: it suggests a residual uncertainty of about 40 MeV. Table 9 shows the value of  $\overline{m}_b(\overline{m}_b)$  for different values of the inputs, using for  $\alpha_s$  a lower scale than  $m_b$  itself,  $M = 2.5 \text{ GeV}$ . The dependence on  $r$  is negligible.

If one computes  $\overline{m}_b$  from  $m_b(1 \text{ GeV})$  at a scale around 3 GeV the perturbative corrections are smaller because the numerical values of the masses get closer. For instance one gets



$\overline{m}_b(2.8 \text{ GeV}) = 4.550 + 0.023_{\alpha_s} - 0.024_{\alpha_s^2} = 4.550$ . This result can be evolved up using four-loop RGE, finding  $\overline{m}_b(\overline{m}_b) = 4.182$ , which is consistent with the values in Table 9 but has arguably a slightly smaller error. Our final estimate is

$$m_b(1 \text{ GeV}) - \overline{m}_b(\overline{m}_b) = (0.37 \pm 0.03) \text{ GeV},$$

The error also includes in quadrature the parametric  $\alpha_s$  error,  $\delta\alpha_s(m_b) = 0.007$ .

## 5 Summary

I have presented the results of a complete  $O(\alpha_s^2)$  calculation of the moments of the lepton energy and hadronic invariant mass distributions in semileptonic  $B \rightarrow X_c \ell \nu$  decays. The numerical Fortran code<sup>4</sup> that has been developed allows us to work in any perturbative scheme; I have adopted the kinetic scheme, but have also considered the option of the  $\overline{\text{MS}}$  scheme for the definition of the charm mass. The non-BLM corrections are generally small and within the expected range. The new code will allow for a NNLO fit to the semileptonic moments, with the possible inclusion of precise mass constraints, in a variety of perturbative schemes. To facilitate the inclusion of mass constraints obtained in the  $\overline{\text{MS}}$  scheme, I have critically reexamined the conversion from that scheme to the kinetic scheme for the heavy quark masses. Additional details concerning the NNLO prediction of the total rate can be found in the Appendix.

I have performed a detailed study of the dependence of the results on various unphysical scales, obtaining useful indications on the size of the residual perturbative uncertainty in the moments, which is now definitely smaller than the uncertainty due to higher dimensional contributions in the OPE and to  $O(\alpha_s)$  contributions to the Wilson coefficients of dimension 5 and 6 operators. Fortunately, work on both these aspects is progressing and there are good prospects for a more accurate prediction of the inclusive semileptonic moments and a more precise determination of  $|V_{cb}|$ .

## Acknowledgements

I am grateful to Paolo Giordano for his contribution in the early stage of this work and to Daniele Papalia for carefully checking many numerical results. I also thank Kirill Melnikov, Alexei Pak, and Einan Gardi for useful communications and discussions, and Kolya Uraltsev for many clarifying conversations and for carefully reading a preliminary version of this paper. Work partly supported by MIUR under contract 2008H8F9RA\_002.

---

<sup>4</sup>The Fortran code is available from [gambino@to.infn.it](mailto:gambino@to.infn.it)

## Appendix

The determination of  $|V_{cb}|$  from inclusive semileptonic  $B$  decays is based on the expression for the charmed total semileptonic width. In this Appendix we update the numerical analysis in the kinetic scheme given in Ref. [5] with the inclusion of the exact two-loop correction computed in [14, 15, 16]. Keeping only terms through  $O(1/m_b^3)$ , the general structure of the width is (see [5] and refs. therein)

$$\Gamma[\bar{B} \rightarrow X_c e \bar{\nu}] = \frac{G_F^2 m_b^5}{192\pi^3} |V_{cb}|^2 g(\rho) (1 + A_{ew}) \left[ 1 + \frac{\alpha_s(m_b)}{\pi} p_c^{(1)}(\rho, \mu) + \frac{\alpha_s^2}{\pi^2} p_c^{(2)}(\rho, \mu) - \frac{\mu_\pi^2}{2m_b^2} + \left( \frac{1}{2} - \frac{2(1-\rho)^4}{g(\rho)} \right) \frac{\mu_G^2 - \frac{\rho_{LS}^3 + \rho_D^3}{m_b}}{m_b^2} + \frac{d(\rho)}{g(\rho)} \frac{\rho_D^3}{m_b^3} \right], \quad (26)$$

where  $\rho = (m_c/m_b)^2$ ,  $g(\rho) = 1 - 8\rho + 8\rho^3 - \rho^4 - 12\rho^2 \ln \rho$ ,  $d(\rho) = 8 \ln \rho - \frac{10\rho^4}{3} + \frac{32\rho^3}{3} - 8\rho^2 - \frac{32\rho}{3} + \frac{34}{3}$ , and all the masses and OPE parameters are defined in the kinetic scheme with cutoff  $\mu$ . The expression for the width is  $\mu$ -independent through  $O(\alpha_s^2)$ . The term  $A_{ew} = 2\alpha/\pi \ln M_Z/m_b \simeq 0.014$  is due to the electromagnetic running of the four-fermion operator from the weak to the  $b$  scale and represents the leading electroweak correction [37].

The results of the two-loop BLM and non-BLM perturbative corrections [10, 15, 16] in the on-shell scheme are well approximated in the relevant mass range by a simple interpolation formula, valid for  $0.17 < r < 0.3$ ,

$$p_c^{(2)}(r, 0) = (-3.381 + 7.15 r - 5.18 r^2) \beta_0 + 7.51 - 21.46 r + 19.8 r^2.$$

Applying these results and the well-known one-loop contribution [39] to the kinetic scheme calculation with  $\mu = 1 \text{ GeV}$ ,  $m_b = 4.6 \text{ GeV}$ , and  $r = 0.25$ , the NNLO perturbative series becomes

$$\Gamma[\bar{B} \rightarrow X_c e \bar{\nu}] \propto 1 - 0.96 \frac{\alpha_s}{\pi} - 0.48 \beta_0 \left( \frac{\alpha_s}{\pi} \right)^2 + 0.81 \left( \frac{\alpha_s}{\pi} \right)^2 \approx 0.916 \quad (27)$$

where  $\beta_0 = 9$  corresponds to three light flavors, and we have used  $\alpha_s(m_b) = 0.22$  for the numerical evaluation. For comparison, Ref. [5] used the same inputs and had  $-1.0$  as coefficient of  $\alpha_s^2$  and the global perturbative factor of Eq. (27) was 0.908. Of course, the difference is due to the recent complete NNLO calculation of [14, 15]. As already discussed, finite charm quark mass effects in the NNLO conversion to the kinetic scheme have not been included. They can be expected to decrease the above value by up to 0.002. Higher order BLM corrections are also known [38] and have been studied in the kinetic scheme where the resummed BLM result is numerically very close to the NNLO one [5]. The residual dependence of the overall perturbative factor on the scale of  $\alpha_s$  is mild: changing it between  $m_b$  and  $m_b/2$  decreases by less than 1%, which represents a reasonable estimate for the residual perturbative uncertainty.

We also provide an approximate formula for  $|V_{cb}|$  in terms of the OPE parameters and  $\alpha_s$ . Using  $\tau_B = 1.582$  ps and  $\text{BR}_{sl,c} = 0.105$  (the measured semileptonic branching ratio after subtraction of  $b \rightarrow ul\nu$  transitions) we have

$$\frac{|V_{cb}|}{0.0416} = 1 + 0.275(\alpha_s - 0.22) - 0.65(m_b - 4.6) + 0.39(m_c - 1.15) + 0.014(\mu_\pi^2 - 0.4) + 0.055(\mu_G^2 - 0.35) + 0.10(\rho_D^3 - 0.2) - 0.012(\rho_{LS}^3 + 0.15), \quad (28)$$

where all dimensionful quantities are expressed in GeV to the appropriate power and are understood in the kinetic scheme with  $\mu = 1$  GeV. The numerical accuracy of this formula is limited to 1% in the  $1\sigma$  range of the current HFAG fits [3]. The combination of  $m_{c,b}$  in the above expression is very similar to the one that appears in the leptonic moments, see Eq. (10).

If the  $\overline{\text{MS}}$  scheme is adopted for the charm mass with  $\overline{m}_c(2 \text{ GeV}) = 1.12$  GeV and  $m_b(1 \text{ GeV}) = 4.6$  GeV, the NNLO perturbative series expressed in terms of  $\alpha_s(m_b)$  becomes

$$\Gamma[\overline{B} \rightarrow X_c e \bar{\nu}] \propto 1 - 1.27 \frac{\alpha_s}{\pi} - 0.33\beta_0 \left(\frac{\alpha_s}{\pi}\right)^2 - 0.29 \left(\frac{\alpha_s}{\pi}\right)^2 \approx 0.895. \quad (29)$$

A simple test of the residual scheme dependence consists in comparing the products of the function  $g(\rho)$  with the overall perturbative factor, Eqs. (27,29), computed in different schemes for  $m_c$ . This product should be scheme independent when the same bottom mass is employed. In the case considered here the values  $m_c(1 \text{ GeV}) = 1.15$  GeV and  $\overline{m}_c(2 \text{ GeV}) = 1.12$  GeV satisfy Eq.(24) and the product is scheme independent to excellent approximation. For a larger  $\overline{\text{MS}}$  scale  $\bar{\mu} = 3$  GeV the perturbative expansion converges slower, but the scheme dependence is well within the 1% uncertainty estimate.

## References

- [1] I. I. Y. Bigi, N. G. Uraltsev and A. I. Vainshtein, Phys. Lett. B **293** (1992) 430 [Erratum-ibid. B **297** (1993) 477] [arXiv:hep-ph/9207214]; I. I. Y. Bigi, M. A. Shifman, N. G. Uraltsev and A. I. Vainshtein, Phys. Rev. Lett. **71** (1993) 496 [arXiv:hep-ph/9304225].
- [2] B. Blok, L. Koyrakh, M. A. Shifman and A. I. Vainshtein, Phys. Rev. D **49** (1994) 3356 [Erratum-ibid. D **50** (1994) 3572] [arXiv:hep-ph/9307247]; A. V. Manohar and M. B. Wise, Phys. Rev. D **49** (1994) 1310 [arXiv:hep-ph/9308246].
- [3] D. Asner *et al.* [Heavy Flavor Averaging Group Collaboration], [arXiv:1010.1589 [hep-ex]], see also <http://www.slac.stanford.edu/xorg/hfag/> .
- [4] I. I. Y. Bigi, M. A. Shifman, N. Uraltsev and A. I. Vainshtein, Phys. Rev. D **56** (1997) 4017 [arXiv:hep-ph/9704245] and Phys. Rev. D **52** (1995) 196 [arXiv:hep-ph/9405410].

- [5] D. Benson, I. I. Bigi, T. Mannel and N. Uraltsev, Nucl. Phys. B **665**, 367 (2003) [hep-ph/0302262].
- [6] P. Gambino and N. Uraltsev, Eur. Phys. J. C **34**, 181 (2004) [hep-ph/0401063].
- [7] D. Benson, I. I. Bigi and N. Uraltsev, Nucl. Phys. B **710**, 371 (2005) [hep-ph/0410080].
- [8] O. Buchmuller, H. Flacher, Phys. Rev. **D73** (2006) 073008. [hep-ph/0507253].
- [9] C. W. Bauer, Z. Ligeti, M. Luke, A. V. Manohar and M. Trott, Phys. Rev. D **70**, 094017 (2004) [hep-ph/0408002].
- [10] V. Aquila, P. Gambino, G. Ridolfi and N. Uraltsev, Nucl. Phys. B **719** (2005) 77 [arXiv:hep-ph/0503083].
- [11] M. Gremm and A. Kapustin, *Phys. Rev.* **D55** (1997) 6924.
- [12] P. Gambino, C. Schwanda, [arXiv:1102.0210 [hep-ex]].
- [13] I. I. Y. Bigi, N. Uraltsev, Int. J. Mod. Phys. **A16** (2001) 5201-5248. [hep-ph/0106346].
- [14] K. Melnikov, Phys. Lett. B **666** (2008) 336 [arXiv:0803.0951 [hep-ph]].
- [15] A. Pak and A. Czarnecki, Phys. Rev. Lett. **100** (2008) 241807 [arXiv:0803.0960 [hep-ph]]; Phys. Rev. **D78** (2008) 114015. [arXiv:0808.3509 [hep-ph]].
- [16] S. Biswas and K. Melnikov, JHEP **1002** (2010) 089 [arXiv:0911.4142 [hep-ph]].
- [17] T. Mannel, S. Turczyk and N. Uraltsev, JHEP **1011**, 109 (2010) [arXiv:1009.4622 [hep-ph]].
- [18] T. Becher, H. Boos and E. Lunghi, JHEP **0712**, 062 (2007) [arXiv:0708.0855 [hep-ph]].
- [19] T. Ewerth, P. Gambino and S. Nandi, Nucl. Phys. B **830** (2010) 278 [arXiv:0911.2175 [hep-ph]].
- [20] M. B. Voloshin, Phys. Rev. **D51** (1995) 4934.
- [21] P. Gambino, P. Giordano, G. Ossola and N. Uraltsev, JHEP **0710** (2007) 058 [arXiv:0707.2493 [hep-ph]]; M. Antonelli *et al.*, Phys. Rept. **494** (2010) 197-414. [arXiv:0907.5386 [hep-ph]].
- [22] P. Gambino, P. Giordano, Phys. Lett. **B669** (2008) 69-73. [arXiv:0805.0271 [hep-ph]].
- [23] K. G. Chetyrkin *et al.*, Phys. Rev. **D80** (2009) 074010 [arXiv:0907.2110 [hep-ph]] and arXiv:1010.6157 [hep-ph].
- [24] B. Dehnadi, A. H. Hoang, V. Mateu, S. M. Zebarjad, [arXiv:1102.2264 [hep-ph]].

- [25] C. McNeile *et al.* [HPQCD Collaboration], *Phys. Rev. D* **82** (2010) 034512 [arXiv:1004.4285 [hep-lat]].
- [26] G. Paz, arXiv:1011.4953 [hep-ph].
- [27] M. Jezabek and J. H. Kuhn, *Nucl. Phys. B* **314** (1989) 1; *Nucl. Phys. B* **320** (1989) 20; A. Czarnecki, M. Jezabek and J. H. Kuhn, *Acta Phys. Polon. B* **20** (1989) 961; A. Czarnecki and M. Jezabek, *Nucl. Phys. B* **427** (1994) 3 [arXiv:hep-ph/9402326].
- [28] M. Gremm and I. Stewart, *Phys. Rev.* **D55** (1997) 1226.
- [29] A. Czarnecki, K. Melnikov and N. Uraltsev, *Phys. Rev. Lett.* **80** (1998) 3189 [arXiv:hep-ph/9708372].
- [30] K. G. Chetyrkin, J. H. Kuhn, M. Steinhauser, *Comput. Phys. Commun.* **133** (2000) 43-65. [hep-ph/0004189].
- [31] A. F. Falk, M. E. Luke, *Phys. Rev.* **D57** (1998) 424-430. [hep-ph/9708327]; A. F. Falk, M. E. Luke, M. J. Savage, *Phys. Rev.* **D53** (1996) 2491-2505 [hep-ph/9507284].
- [32] M. Trott, *Phys. Rev. D* **70** (2004) 073003 [arXiv:hep-ph/0402120].
- [33] N. Uraltsev, *Int. J. Mod. Phys. A* **20** (2005) 2099 [arXiv:hep-ph/0403166].
- [34] K. Melnikov, private communication.
- [35] K. G. Chetyrkin, M. Steinhauser, *Nucl. Phys.* **B573** (2000) 617-651. [hep-ph/9911434]; K. Melnikov, T. v. Ritbergen, *Phys. Lett.* **B482** (2000) 99-108 [hep-ph/9912391].
- [36] N. Gray, D. J. Broadhurst, W. Grafe, K. Schilcher, *Z. Phys.* **C48** (1990) 673-680.
- [37] A. Sirlin, *Nucl. Phys. B* **196** (1982) 83.
- [38] P. Ball, M. Beneke and V. M. Braun, *Phys. Rev. D* **52** (1995) 3929 [arXiv:hep-ph/9503492]; see also N. Uraltsev, *Nucl. Phys.* **B491** (1997) 303-322 [hep-ph/9610425] and Ref. [5].
- [39] Y. Nir, *Phys. Lett. B* **221** (1989) 184.